Zentrum für Technomathematik
Fachbereich 3 – Mathematik und Informatik

Length scales in the concrete carbonation process and water barrier effect: a matched asymptotics approach

Adrian Muntean **Michael Böhm**

Report 06–07

Berichte aus der Technomathematik

Report 06–07 **September 2006**

LENGTH SCALES IN THE CONCRETE CARBONATION PROCESS AND WATER BARRIER EFFECT: A MATCHED ASYMPTOTICS APPROACH

ADRIAN MUNTEAN AND MICHAEL BÖHM

ABSTRACT. The reaction $CO_2 + Ca(OH)_2 \to H_2O + CaCO_3$ takes place in unsaturated porous concrete-based materials with separated reactants, where CO_2 and H_2O are diffusing and $Ca(OH)_2$ can be assumed as immobile. The process (called carbonation) plays an important role in the service life of concrete-based structures. Our aims are threefold:

(1) We study via a matched-asymptotics approach the *occurrence of two distinct length scales* in the carbonation process. These scales are arising due to the strong competition between reaction and diffusion effects. We show that for sufficiently large times τ the width of the carbonated region is proportional to $\sqrt{\tau}$, while the width of the reaction front is proportional to $\tau^{\frac{p-1}{2(p+1)}}$ for carbonation-reaction rates with a power law structure like $k[CO_2]^p[Ca(OH)]_2^q$, where $k > 0$ and $p, q > 1$.

(2) We emphasize the occurrence of a *water barrier* in the reaction zone which may hinder the penetration of CO_2 by locally filling with water air parts of the pores. This *non-linear effect* may be one of the causes why a purely linear extrapolation of accelerated carbonation test results to natural carbonation settings is (even theoretically) not reasonable.

(3) We compare the *asymptotic penetration law*, which we obtain for the position of the reaction front, against measured penetration depths from [5]. The novelty consists in the fact that the factor multiplying $\sqrt{t}$ is now identified asymptotically by solving a non-linear system of ordinary differential equations, and hence, no fitting arguments are necessary to estimate its size. Our law is an alternative to the asymptotic $\sqrt{t}$ expression of the carbonation-front position obtained by Papadakis, Vayenas and Fardis in [26].

Key words: reaction-diffusion process, concrete carbonation, separation of length scales, water barrier, asymptotic penetration law, matched asymptotics

1. INTRODUCTION

The reaction-diffusion process studied in this note concerns the following scenario: The mechanism

$$CO_2(g \to aq) + Ca(OH)_2(s \to aq) \to H_2O + CaCO_3(aq \to s) \tag{1.1}$$

takes place in unsaturated porous concrete-based materials, where the reactants are assumed to be initially separated. The physicochemical process associated with (1.1) can be described as follows: CO_2 from the atmosphere penetrates the concrete material via the air parts of the pores and get absorbed in pore water. Once arrived in pore water, aqueous CO_2 moves to the places where aqueous $Ca(OH)_2$ is available. The latter species comes from the pore matrix via dissolution. The reactants meet and react cf. (1.1) to produce moisture (H_2O) and carbonates ($CaCO_3$). The process is called carbonation and plays an important role in the service life of concrete-based structures. For more details on concrete carbonation and its relevance with respect to corrosion and durability issues of concrete-based structures, we refer the reader to the surveys by Kropp [14] and Chaussadent [7] as well as to the references cited therein.

In this paper, we rely on a conceptually simple isoline model to investigate a couple of asymptotic features of the carbonation process. The particularities of this model, which has been presented in [6] and is reformulated with minor modifications in section 2, are the following: The reactant CO_2 and the product H_2O are allowed to diffuse, while the the other reactant $Ca(OH)_2$ is static. Furthermore, we assume that the total porosity of the concrete stays constant. Despite its apparent simplicity, the model encompasses the main features of the carbonation process. More elaborate models were proposed by several authors, see for instance [13, 27, 32, 21]. In the sequel, we focus on the following issues:

(1) We study the *asymptotic separation of length scales* during carbonation arisen due to the strong competition between reaction and diffusion effects. We show that for sufficiently large times τ the width of the carbonated region is proportional to $\sqrt{\tau}$, while the width of the reaction front is proportional to $\tau^{\frac{p-1}{2(p+1)}}$ for carbonation-reaction rates with a power law structure like $k[CO_2]^p[Ca(OH)]_2^q$, where $k > 0$ and $p, q > 1$. The same issue was touched, for instance, in [28, 8, 4, 15, 36] from both theoretical and experimental viewpoints.
(2) We emphasize the occurrence of a *water barrier* in the reaction zone which, under certain circumstances, can hinder the penetration of CO_2 by locally filling with water the air parts of the pores. This *non-linear effect* may be one of the causes why a purely linear extrapolation of accelerated carbonation test results to natural carbonation settings is not possible. Our motivation for this subject was explained in detail in [25]. At that point, we have listed a set of non-linear issues which can hinder any reasonable *a priori* quantitative extrapolation in correct ranges.
(3) We compare the *asymptotic penetration law*, which we obtain for the description of the position of the reaction front, against measured penetration depths extracted from Bunte's PhD thesis [5]. The novelty consists in the fact that the factor multiplying $\sqrt{t}$ is now identified asymptotically by solving a non-linear system of ordinary differential equations, and hence, no fitting arguments are necessary to estimate its size. Our law may be viewed as another asymptotic alternative to the asymptotic $\sqrt{t}$ expression of the reaction-front position in [26]. In contrast to [26], we do not shrink the reaction layer to the corresponding *free boundary*. We rather prefer to keep the geometry of the layer as it is and estimate its width asymptotically taking into account the structure of the reaction kinetics.

Our motivation to apply formal asymptotic methods in order to to tackle subjects like those stated in (1)-(3) basically stems from the pioneering approach to carbonation by Papadakis, Vayenas and Fardis in [26]. At the modeling level, we are influenced by the asymptotic investigation of $Ca(OH)_2$ leaching in concrete done by Mainguy in his PhD thesis [18] and then applied in [19] by Mainguy and Coussy to the same problem. Similar ideas as in [18] were employed in the context of carbonation by Thiéry in his PhD thesis [35]. At the technical level, since we employ matched asymptotics (see [2, 29, 16, 34], e.g., for details), our approach is different. The mathematical core of this contribution follows partly the lines of the paper by Bazant and Stone [4]. We apply some of their ideas to the carbonation problem. Nevertheless, the introduction of an additional partial differential equation to describe the diffusive behavior of the moisture produced by reaction (1.1), and also, our particular choice of scaling parameters used to non-dimensionalize the model equations lead us away from the basic framework treated in [4]. Since in the interior of the reaction layer the equation of moisture formally decouples from those of

the reactants, many of the working ideas employed in [4] become applicable to our setting.

The paper is organized as follows:

Contents

2. Carbonation model

We consider the carbonation model as proposed by Cahyadi and Uomoto in [6]. One of the particularities of their formulation is that the molecules of $Ca(OH)_2$ and $CaCO_3$ are supposed to be immobile (non-diffusing), while those of CO_2 and of moisture may diffuse. Moreover, we consider that production and precipitation of $CaCO_3$ are equal and do not significantly affect the remaining mechanisms of the reaction-diffusion problem in question.

Denote by u, v and w the dimensionless concentration of CO_2(aq), $Ca(OH)_2$(aq) and moisture produced by the reaction

$$CO_2 + Ca(OH)_2 \to H_2O + CaCO_3. \tag{2.1}$$

Note that there are a few conceptual differences between (1.1) and (2.1). Particularly, in the sequel we do not distinguish between the water and air phases. The main reason which is behind such a treatment is that both the transfer of CO_2 from the air to water phase (and *vice versa*) and the dissolution of $Ca(OH)_2$ from the solid matrix to water phase (and *vice versa*) may be assumed to be in local equilibrium. Let $\Omega :=]-\infty, +\infty[$ and $S :=]0, \infty[$ be the space and time domain of

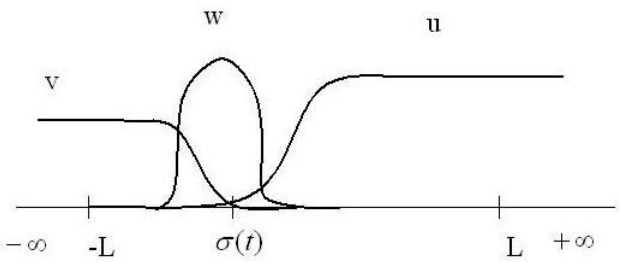

Figure 1. Typical behavior of active concentrations u, v and w.

interest. Our choice of Ω underlines the fact that we do not account for boundary

effects. Following [26, 23], the carbonation problem may be stated in dimensionless form as

$$u_{,\tau} - \delta_u u_{,zz} = -\Phi^2 f(u,v) \text{ equation for } CO_2 \tag{2.2}$$

$$\beta_v v_{,\tau} = -\Phi^2 f(u,v) \text{ equation for } CaOH_2 \tag{2.3}$$

$$\beta_w w_{,\tau} - \delta_w w_{,zz} = +\Phi^2 f(u,v) \text{ equation for } H_2O \tag{2.4}$$

$$u(z,0) = H(z), v(z,0) = H(-z) \text{ and } w(z,0) = 0 \text{ for all } z \in \Omega, \tag{2.5}$$

$$u(\infty,\tau) = 1 \text{ and } w(\infty,\tau) = \hat{w}, u(-\infty,\tau) = 0, w(-\infty,\tau) = \hat{w} \text{ for all } \tau \in S. \tag{2.6}$$

We are looking for left-traveling *wave fronts* of CO_2 and $Ca(OH)_2$ concentrations and for a *pulse* of humidity, see Fig. 1. These are solutions defined on the entire real line (see chapter 3 in [17], e.g.) and represent a mathematical ansatz of wave concentration profiles in the laboratory or *in situ* experiment. By (2.6), the wave of CO_2 is a compression (contamination) wave, while that of $Ca(OH)_2$ is a rarefaction (remediation) one.

The parameters δ_u, δ_w, β_v, β_w and Φ^2 are positive quantities which correspondingly represent the effective CO_2 and humidity diffusivities, impact capacity factors, and the Thiele modulus, see section 8 for typical values. The term

$$f(u,v) := u^p v^q \tag{2.7}$$

denotes the production by carbonation reaction. Note that the mass-balance equations are coupled by means of f. In (2.5), $H(\cdot)$ is the Heaviside function which is defined by

$$H(\zeta) = \begin{cases} 0, & \text{if } \zeta < 0, \\ 1, & \text{if } \zeta \geq 0. \end{cases} \tag{2.8}$$

For simplicity, we assume in (2.6) that $\hat{w} = 0$. Therefore, w comprises only the concentration of water produced by (1.1). Furthermore, since the species whose concentration is denoted by v is not allowed to diffuse, it cannot leave its initial support, and hence, $v(x,t) = 0$ for all $x > 0$ and $t \geq 0$. The reactant u diffuses into $-x$ direction toward the place hosting the static reactant v. Arguing as in [2, 4], if an asymptotic similarity solution exist, then it must involve a moving front which *diffuses* into the material. See section 3 and [3, 26, 4, 15], e.g., for discussions concerning *why* such a front is expected to exist. We denote by $\sigma(\tau)$ its position at the moment $\tau > 0$. For fixing the ideas, let $\sigma(\tau)$ be the center of the reaction zone. We assume that $\frac{d\sigma(\tau)}{d\tau} < 0$, where $\sigma(\tau)$ is given by

$$\sigma(\tau) := -2m\tau^\alpha, \alpha \in \mathbb{R}, \tau \geq 0. \tag{2.9}$$

The coefficient m is *a priori unknown*. We expect m to depend on the Thiele modulus Φ^2, but the precise way in which this dependence holds still needs to be identified. We address the determination of m in section 7. The dependence of m on Φ^2 is explained for a particular case in section 9. In the sequel, we omit to write down explicitly the dependence of m on Φ^2.

We use the definition (2.9) of $\sigma(\tau)$ in order to distinguish between the three space domains of interest. Namely, we denote the carbonated zone (also called *diffusion layer*), the inter-phase carbonation layer (called also *reaction layer*) and the uncarbonated part, respectively, by

$$\Omega_1(\tau) :=]\sigma(\tau) + \epsilon/2, \infty[, \tag{2.10}$$

$$\Omega_\epsilon(\tau) := [\sigma(\tau) - \epsilon/2, \sigma(\tau) + \epsilon/2], \tag{2.11}$$

$$\Omega_2(\tau) :=]-\infty, \sigma(\tau) - \epsilon/2[, . \tag{2.12}$$

By (2.12), ϵ is the width of $\Omega_\epsilon(\tau)$. In this framework, $\Omega_\epsilon(\tau)$ some sort of *a mushy region* where u, v and w coexist. Since $\frac{d\sigma}{d\tau} < 0$, the reaction front $\Omega_\epsilon(\tau)$ (and implicitely the production by reaction $f(u,v)$) *moves* towards the location of the source of v. The separation of reactants can be expressed as

$$u(z,\tau) = 0 \text{ for all } z \in \Omega_2(\tau), \tag{2.13}$$

$$v(z,\tau) = 0 \text{ for all } z \in \Omega_1(\tau). \tag{2.14}$$

Furthermore, we have

$$w(z,\tau) = 0 \text{ for all } z \in \Omega_1(\tau) \cup \Omega_2(\tau). \tag{2.15}$$

3. Inner problem

We consider as *inner problem* the scaling of the reaction layer $\Omega_\epsilon(\tau)$. We make use of the stretching variable

$$\eta := \frac{z + \sigma(\tau)}{\tau^\beta} = \frac{z + 2m\tau^\alpha}{\tau^\beta}, \tag{3.1}$$

where we assume that the width ϵ of $\Omega_\epsilon(\tau)$ is proportional to τ^β fo *some* $\beta \geq 0$. By (3.1), we deduce

$$\eta_{,z} = \tau^{-\beta} \text{ and } \eta_{,\tau} = -\beta\tau^{-1}\eta + 2m\alpha\tau^{\alpha-\beta-1}. \tag{3.2}$$

In the vicinity of $\sigma(\tau)$, we allow the concentrations u and w to vary like

$$U(\eta,\tau) := \tau^\gamma u(z,\tau), V(\eta,\tau) = v(x,t) \text{ and } W(\eta,\tau) = \tau^\nu w(z,\tau) \tag{3.3}$$

with $\gamma > 0$ and $\nu > 0$. We refer the reader to [4], for a discussion of the non-relevance of the cases $\gamma = 0$ and $\nu = 0$.

Owing to (3.3), it is necessary to replace $f(u,v)$ in (2.7) by $f(U,V) = \tau^{-\delta}U^pV^q$, with $\delta := \gamma p$.

By (3.1), (3.2), 3.3) and the chain rule, the mass-balance equations (2.2), (2.3) and (2.4) become

$$\begin{aligned}\tau^{\gamma(p-1)}U_{,\tau} - \tau^{\gamma(p-1)-1}\left(\beta\eta U_{,\eta} + \gamma U\right) + 2m\alpha\tau^{\alpha-\beta+\gamma(p-1)-1}U_{,\eta} = \\ \tau^{\gamma(p-1)-2\beta}\delta_u U_{,\eta\eta} - \Phi^2 U^pV^q,\end{aligned} \tag{3.4}$$

$$\tau^{\gamma p}V_{,\tau} - \tau^{\gamma p-1}\beta\eta V_{,\eta} + 2m\alpha\tau^{\alpha-\beta+\gamma p-1}V_{,\eta} = -\frac{\Phi^2}{\beta_v}U^pV^q, \tag{3.5}$$

$$\begin{aligned}\tau^{\gamma p-\nu}W_{,\tau} - \tau^{\gamma p-\nu-1}\left(\beta\eta W_{,\eta} + \nu W\right) + 2m\alpha\tau^{\alpha-\beta+\gamma p-\nu-1}W_{,\eta} = \\ \tau^{p\gamma-\nu-2\beta}\frac{\delta_w}{\beta_w}W_{,\eta\eta} + \frac{\Phi^2}{\beta_w}U^pV^q.\end{aligned} \tag{3.6}$$

We aim at finding asymptotically invariant (similarity) solutions which correspond to the following limiting behavior with suitable $\hat{U}$, $\hat{V}$ and $\hat{W}$:

$$\begin{aligned} U(\eta,\tau) \to \hat{U}(\eta), \quad V(\eta,\tau) \to \hat{V}(\eta), \quad W(\eta,\tau) \to \hat{W}(\eta), \\ U_{,\eta}(\eta,\tau) \to \hat{U}_{,\eta}(\eta), \quad V_{,\eta}(\eta,\tau) \to \hat{V}_{,\eta}(\eta), \quad W_{,\eta}(\eta,\tau) \to \hat{W}_{,\eta}(\eta), \\ U_{,\eta\eta}(\eta,\tau) \to \hat{U}_{,\eta\eta}(\eta), \quad W_{,\eta\eta}(\eta,\tau) \to \hat{W}_{,\eta\eta}(\eta)\end{aligned} \tag{3.7}$$

as $\tau \to \infty$ and $-\infty < \eta < \infty$. We make use of the same arguments as in [4] to require the presence of a *dominant balance* (cf. also chapter 5 in [12]), which compensates the effect of the nonlinear reaction U^pV^q. The first step needed in order to obtain the time-invariance of U, V and W is to require the smallness of the terms $U_{,\tau}$, $V_{,\tau}$ and $W_{,\tau}$ relatively to the production by reaction. In other words, we assume the *pseudo-steady state approximation* for U, V and W, i.e.

$$\lim_{\tau\to\infty}\tau^{\gamma(p-1)}U_{,\tau} = \lim_{\tau\to\infty}\tau^{\gamma p}V_{,\tau} = \lim_{\tau\to\infty}\tau^{\gamma p-\nu}W_{,\tau} = 0. \tag{3.8}$$

The dominant balance situations for U, V, and W suggest the study of the following cases:

$$\begin{aligned}
&(U1)\ \gamma(p-1)-2\beta=0, \quad \alpha-\beta+\gamma(p-1)-1\le 0, \quad \gamma(p-1)-1\le 0,\\
&(U2)\ \gamma(p-1)-2\beta\le 0, \quad \alpha-\beta+\gamma(p-1)-1= 0, \quad \gamma(p-1)-1\le 0,\\
&(U3)\ \gamma(p-1)-2\beta\le 0, \quad \alpha-\beta+\gamma(p-1)-1\le 0, \quad \gamma(p-1)-1= 0,
\end{aligned}$$

$$\begin{aligned}
&(V1)\ \gamma p-1=0, \quad \alpha-\beta+\gamma p-1\le 0,\\
&(V2)\ \gamma p-1\le 0, \quad \alpha-\beta+\gamma p-1= 0,
\end{aligned}$$

and

$$\begin{aligned}
&(W1)\ p\gamma-\nu-2\beta=0, \quad \alpha-\beta+\gamma p-\nu-1\le 0, \quad \gamma p-\nu-1\le 0,\\
&(W2)\ p\gamma-\nu-2\beta\le 0, \quad \alpha-\beta+\gamma p-\nu-1= 0, \quad \gamma p-\nu-1\le 0,\\
&(W3)\ p\gamma-\nu-2\beta\le 0, \quad \alpha-\beta+\gamma p-\nu-1\le 0, \quad \gamma p-\nu-1= 0.
\end{aligned}$$

We proceed as in [4] and find out the traveling wave cases (U2, V2, W1) and (U2, V2, W2) and the diffusing front case (U1, V2, W1). We drop those configurations which are not logically consistent[1], see appendix A for details. We are not interested in any traveling wave, but only on those that are bounded and approach constant, equilibrium states at $z=\pm\infty$. These special types of traveling wave solutions are called wave front (or diffusing front) solutions. On this way, we are only left with the diffusing front case (U1,V2,W1). Therefore, we are forced to take into account two regions with different scale invariance: one for the *diffusion layer*, and another one for the *reaction layer*. In this case the front advances sub-linearly in time, i.e. like t^α with $0<\alpha<1$. Note that such a sub-linear behavior of the front has been mathematically shown for two moving-boundary formulations of the concrete carbonation problem in [23].

4. Outer problem

In this section, we deal with the case of the infinitely thin carbonation front (layer). Namely, we only consider the case when Thiele modulus $\Phi^2 \gg 1$ is and finite, see appendix A in [23] or [26], e.g. We are motivated to study this case by the fact that during the carbonation process the reaction is *faster* than the transport. Therefore, we expect that the width $\epsilon>0$ of the reaction layer $\Omega_\epsilon(\tau)$ is relatively small compared to the width of the diffusion layer $\Omega_1(\tau)$. Such setting occurs when in the reaction-diffusion process the characteristic time scale of reaction is much smaller than that of diffusion.

We consider as *outer problem* the scaling of the diffusion layer $\Omega_1(\tau)$. To scale this region, we introduce another similarity variable which reads

$$\zeta := \frac{2m\tau^\alpha + z}{2\tau^\rho} \text{ for all } \zeta>0,\ zeta\ge\sigma. \tag{4.1}$$

In (4.1), we have $\rho>0$. The similarity variables η cf. (3.1) and ζ cf. (4.1) are linked through

$$\eta = 2\tau^{\rho-\beta}\zeta.$$

If $\eta\to\infty$ and $\zeta\to 0$ with $\zeta>0$, then the carbonated zone needs to connect with the reaction layer. Let us introduce some new functions

$$\mathcal{U}(\zeta,\tau) := u(z,\tau),\ \mathcal{V}(\zeta,\tau) := v(z,\tau) \text{ and } \mathcal{W}(\zeta,\tau) := w(z,\tau). \tag{4.2}$$

[1]For the case (U1, V2, W1), we have $\nu=\gamma$, $0<\gamma\le\frac{1}{p}$, $\beta=\frac{\gamma}{2}(p-1)$, $\alpha\le 1-\frac{\gamma}{2}(p-1)$. The same arguments as in [4] can be used to show that the traveling wave ansatz is not satisfactory for the reaction-diffusion model in question. We do not repeat them here and refer the reader to (22a)-(23) in [4].

As in section 3, we omit to write the dependence of m on Φ^2. (4.1) yields

$$\zeta_{,z} = \frac{1}{2\tau^\rho} \text{ and } \zeta_{,\tau} = m\alpha\tau^{\alpha-\rho-1} - \zeta\rho\tau^{-1}. \tag{4.3}$$

The mass-balance equations (2.2)-(2.4) become

$$\tau^{2\rho}\mathcal{U}_{,\tau} + m\alpha\tau^{\alpha+\rho-1}\mathcal{U}_{,\zeta} - \zeta\rho\tau^{2\rho-1}\mathcal{U}_{,\zeta} = \frac{1}{4}\delta_u\mathcal{U}_{\zeta\zeta} - \Phi^2\tau^{2\rho}\mathcal{U}^p\mathcal{V}^q, \tag{4.4}$$

$$\tau^{2\rho}\mathcal{V}_{,\tau} + m\alpha\tau^{\alpha+\rho-1}\mathcal{V}_{,\zeta} - \zeta\rho\tau^{2\rho-1}\mathcal{V}_{,\zeta} = -\frac{\Phi^2}{\beta_v}\tau^{2\rho}\mathcal{U}^p\mathcal{V}^q, \tag{4.5}$$

and

$$\tau^{2\rho}\mathcal{W}_{,\tau} + m\alpha\tau^{\alpha+\rho-1}\mathcal{W}_{,\zeta} - \zeta\rho\tau^{2\rho-1}\mathcal{W}_{,\zeta} = \frac{1}{4}\frac{\delta_u}{\beta_w}\mathcal{W}_{\zeta\zeta} - \frac{\Phi^2}{\beta_w}\tau^{2\rho}\mathcal{U}^p\mathcal{V}^q. \tag{4.6}$$

We look for capturing the following asymptotic similarity behavior

$$\begin{aligned}
&\mathcal{U}(\zeta,\tau)\to\hat{\mathcal{U}}(\zeta), \quad &&\mathcal{V}(\zeta,\tau)\to\hat{\mathcal{V}}(\zeta), \quad &&\mathcal{W}(\zeta,\tau)\to\hat{\mathcal{W}}(\zeta),\\
&\mathcal{U}_{,\zeta}(\zeta,\tau)\to\hat{\mathcal{U}}_{,\zeta}(\zeta), \quad &&\mathcal{V}_{,\zeta}(\zeta,\tau)\to\hat{\mathcal{V}}_{,\zeta}(\zeta), \quad &&\mathcal{W}_{,\zeta}(\zeta,\tau)\to\hat{\mathcal{W}}_{,\zeta}(\zeta),\\
&\mathcal{U}_{,\zeta\zeta}(\zeta,\tau)\to\hat{\mathcal{U}}_{,\zeta\zeta}(\zeta), \quad &&\mathcal{W}_{,\zeta\zeta}(\zeta,\tau)\to\hat{\mathcal{W}}_{,\zeta\zeta}(\zeta),
\end{aligned}$$

as $\tau\to\infty$ and $\zeta>0$. In order to realize this, we firstly assume that the time derivative of $\mathcal{U}$, $\mathcal{V}$ and $\mathcal{W}$ can be neglected when compared to diffusion terms

$$\lim_{\tau\to\infty}\tau^{2\rho}\mathcal{U}_{,\tau}(\zeta,\tau) = \lim_{\tau\to\infty}\tau^{2\rho}\mathcal{W},\tau(\zeta,\tau) = 0 \text{ for all } \zeta>0. \tag{4.7}$$

A scaling, which is *different* from that one used for the carbonation layer, can be acquired if the production by reaction does not enter the dominant balance. Thus, we assume that

$$\lim_{\tau\to\infty}\tau^{2\rho}\Phi^2\mathcal{U}^p(\zeta,\tau)\mathcal{V}^q(\zeta,\tau) = 0 \text{ for all } \zeta>0. \tag{4.8}$$

The investigation of the dominant balance suggests the following possible cases:

$$\begin{aligned}
&\alpha+\rho-1=0, \quad 2\rho-1\le 0\\
&\alpha+\rho-1\le 0, \quad 2\rho-1=0.
\end{aligned}$$

The situation corresponding to $\alpha+\rho-1\le 0$ and $2\rho-1=0$ represents the case of the diffusing front-like solution, the width of the carbonated region being then proportional to $\sqrt{\tau}$. The other situation is eliminated as in [4].

5. Matching of the inner and outer approximations

The limit $\eta\to\infty$ of the inner approximation has to match the limit $\zeta\to 0, \zeta>0$ of the outer approximation. Since we want to obtain an asymptotic matching, it is essential to pass to the limit $\tau\to\infty$ before the matching is realized. The major care is to propose those matching conditions which conserve the mass when passing from the diffusion layer to the reaction layer.

The matching of v is

$$\lim_{\eta\to\infty}\hat{V}(\eta) = 0 = \lim_{\zeta\to 0^+}\hat{\mathcal{V}}(\zeta). \tag{5.1}$$

To match the outer and inner limits of u and w, some care is needed to formulate the connecting conditions in the *intermediate zone*. This intermediate region lies between the reaction and diffusion layer. Note firstly that since $\gamma>0$ the concentration profiles of u and w decay to zero as $t\to\infty$ and $|\eta|<\infty$. The decay happens like $u(z,\tau)=\mathcal{O}(\tau^{-\gamma})$ and $w(z,\tau)=\mathcal{O}(\tau^{-\nu})$. We proceed as in [4] and match the

linear terms in the Taylor expansion of u and w in the intermediate region. Notice that

$$u_{,z}(z,\tau)=\frac{\hat{\mathcal{U}}'(\zeta)}{2\tau^{\rho}},\ w_{,z}(z,\tau)=\frac{\hat{\mathcal{W}}'(\zeta)}{2\tau^{\rho}}, \tag{5.2}$$

as $\tau\to\infty$ and $0<\zeta<\infty$ is fixed, and

$$u_{,z}(z,\tau)=\frac{1}{\tau^{\beta+\gamma}}\hat{U}'(\eta),\ w_{,z}(z,\tau)=\frac{1}{\tau^{\beta+\nu}}\hat{W}'(\eta), \tag{5.3}$$

as $\tau\to\infty$ and $|\eta|<\infty$ is fixed. (5.2) and (5.3) suggest the matching of the exponents

$$\beta+\gamma=\rho,\quad \beta+\nu=\rho \tag{5.4}$$

and also

$$\hat{U}'(\infty)=\frac{1}{2}\hat{\mathcal{U}}'(0),\quad \hat{W}'(\infty)=\frac{1}{2}\hat{\mathcal{W}}'(0). \tag{5.5}$$

The values of $\hat{U}'(\infty)$ and $W'(\infty)$ will be calculated in section 6. Finally, we conclude this section by giving the asymptotic scaling we were looking for:

$$\beta=\frac{p-1}{2(p+1)},\ \gamma=\frac{1}{p+1},\ \rho=\alpha=\frac{1}{2},\ \delta=\frac{p}{p+1}=p\gamma, \tag{5.6}$$

and recall the relation $\nu=\gamma$. It is worth mentioning that the value of γ in (5.6) is obtained combining

$$\beta+\gamma=\rho \text{ and } \beta=\frac{\gamma}{2}(p-1).$$

6. Calculation of $\hat{U}'(\infty)$ and $\hat{W}'(\infty)$

The concentration profiles of $\hat{U}$ and $\hat{W}$ can be calculated in the diffusion layer. Herein, we have

$$2(m-\zeta)\hat{U}'=\delta_u\hat{U}''$$
$$\hat{U}(0)=0,\ \hat{U}(\infty)=1$$

and hence,

$$-2\left(\frac{\zeta}{\delta_u}-\frac{m}{\delta_u}\right)\hat{U}'=\hat{U}'' \tag{6.1}$$

$$\hat{U}(0)=0,\ \hat{U}(\infty)=1. \tag{6.2}$$

The exact solution of (6.1)-(6.2) is

$$\hat{U}(\zeta)=\frac{\operatorname{erf}\left(\frac{\zeta}{\delta_u}-\frac{m}{\delta_u}\right)+\operatorname{erf}\left(\frac{m}{\delta_u}\right)}{1+\operatorname{erf}\left(\frac{\mathrm{m}}{\delta_{\mathrm{u}}}\right)}, \tag{6.3}$$

where the error function erf is defined by

$$\operatorname{erf}(\lambda)=\frac{2}{\sqrt{\pi}}\int_0^{\lambda}\exp(-r^2)dr$$

for all $\lambda\geq 0$. Similarly, we obtain

$$\hat{W}(\zeta)=0 \text{ for all } \zeta\geq 0. \tag{6.4}$$

Denoting

$$M_u:=\frac{m}{\delta_u} \text{ and } \alpha:=\frac{\zeta}{\delta_u}, \tag{6.5}$$

we can write

$$\frac{U'(0)}{2} = \lim_{\zeta\to 0}\frac{\hat{U}'(\zeta)}{2} = \lim_{\zeta\to 0}\frac{1}{\sqrt{\pi}\,(1+\operatorname{erf}(M_u))}\exp\left(-(\alpha-M_u)^2\right), \tag{6.6}$$

$$\frac{W'(0)}{2} = \lim_{\zeta\to 0}\frac{\hat{W}'(\zeta)}{2} = 0. \tag{6.7}$$

The matching conditions allow us to define U^* and W^* via

$$U^* = \hat{U}'(\infty) = \frac{U'(0)}{2}, \tag{6.8}$$

$$W^* = \hat{W}'(\infty) = \frac{W'(0)}{2}. \tag{6.9}$$

7. Identification of m in (2.9)

Let us consider the following system of ordinary differential equations which hold in the reaction front:

$$\delta_u\hat{\mathcal{U}}'' - \Phi^2\hat{\mathcal{U}}^p\hat{\mathcal{V}}^q = 0, \tag{7.1}$$

$$m\hat{\mathcal{V}}' - \frac{\Phi^2}{\beta_v}\hat{\mathcal{U}}^p\hat{\mathcal{V}}^q = 0, \tag{7.2}$$

$$\delta_w\hat{\mathcal{W}}'' + \frac{\Phi^2}{\beta_w}\hat{\mathcal{U}}^p\hat{\mathcal{V}}^q = 0. \tag{7.3}$$

The associated boundary conditions are

$$\hat{\mathcal{U}}(-\infty) = 0 \quad \hat{\mathcal{U}}'(\infty) = U^*, \tag{7.4}$$

$$\hat{\mathcal{V}}(-\infty) = 1 \qquad \hat{\mathcal{V}}(\infty) = 0, \tag{7.5}$$

$$\hat{\mathcal{W}}(-\infty) = 0 \quad \hat{\mathcal{W}}'(\infty) = W^*, \tag{7.6}$$

where the boundary values U^* and W^* are given by (6.8) and (6.9). It is important to observe that we need all 6 boundary conditions listed in (7.4)-(7.6) in order to find the solution $\hat{\mathcal{U}}$, $\hat{\mathcal{V}}$ and $\hat{\mathcal{W}}$ of the system (7.1)-(7.3), and simultaneously, to identify the parameter m. Note that $\hat{\mathcal{U}}$, $\hat{\mathcal{V}}$, $\hat{\mathcal{W}}$ and m depend on the choice of δ_w, β_v, β_w and Φ^2. Combining[2] equations (7.4) and (7.5) and then integrating the result firstly from t up to ∞, and afterwards, integrating the result mentioned above from $-\infty$ up to t yields

$$\delta_u U^* - \delta_u\hat{\mathcal{U}}'(t) - \beta_v m\hat{\mathcal{V}}(t) = 0 \text{ and } -\beta_v m + \beta_v m\hat{\mathcal{V}}(t) + \delta_u\hat{\mathcal{U}}'(t) = 0, \tag{7.7}$$

for all $t \geq 0$, and hence,

$$m = \frac{\delta_u U^*(m)}{\beta_v}. \tag{7.8}$$

(7.8) has a uniquely determined solution $m > 0$, see Fig. 2. This type of reasoning is standard if we think of calculating wave speeds. With the notation

$$\Theta : [0,\infty[\to\mathbb{R} \text{ defined by } \Theta(\chi) := \frac{1}{\beta_v}\left[\frac{e^{-\chi^2}}{\sqrt{\pi}(1+\operatorname{erf}(\chi))}\right], \tag{7.9}$$

we get $U^*(\chi) = \beta_v\Theta(\chi)$ for all $\chi \geq 0$. It is straightforward to eliminate $\hat{\mathcal{V}}$ to obtain a single equation in terms of $\hat{\mathcal{U}}$. By (7.1), (7.2) and (7.7), we obtain

$$\hat{\mathcal{U}}'(t) = U^* - \frac{\beta_v m}{\delta_u}\hat{\mathcal{V}}(t) = U^*(1-\hat{\mathcal{V}}(t)) \text{ for } t \geq 0, \tag{7.10}$$

[2]See also [17] pp. 78-79, e.g.

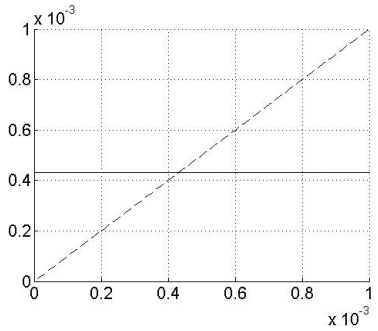

FIGURE 2. Calculation of m for the standard set of parameters used in section 8. The dotted line is the l.h.s. of (7.8), while the solid line is the corresponding r.h.s.

and hence,

$$\hat{\mathcal{V}}(t) = 1 - \frac{\hat{\mathcal{U}}(t)}{U^*}, t \geq 0. \tag{7.11}$$

Thus (7.1) becomes

$$\delta_u \hat{\mathcal{U}}'' - \Phi^2 \hat{\mathcal{U}}^p \left(1 - \frac{\hat{\mathcal{U}}'}{U^*}\right)^q = 0. \tag{7.12}$$

The boundary conditions (7.4) are associated to the non-linear equation (7.12). Questions concerning the existence and uniqueness of the reaction front scaling function $\hat{\mathcal{U}}$, which satisfies (7.12) and (7.4), were addressed in [4], section 3.6. Once $\hat{\mathcal{U}}$ is known, the system (7.1)-(7.6) decouples and the remaining equations are then easy to integrate.

8. Simulation results

We turn our attention to the carbonation setting described in [5]. We perform the calculations with respect to the space domain $\Omega_L :=]-L, L[$ and the time interval $S_T :=]0, T[$. In this section, we set $L = 1$ cm, $\epsilon = \frac{1}{7}$ cm and $T = 18$ years. Note that T represents the final time of the carbonation process in Bunte's experiment (cf. [5]) and $L > \epsilon$. The couple (Ω_L, S_T) is used for the numerical approximation of the *infinitely* large intervals Ω and S. Further, let us denote by D_A the effective diffusivity of species A, by λ_A the Dirichlet boundary datum which we assume to be compatible with the corresponding initial datum. Our candidates for A are the reactants and products involved in (1.1). By $\eta_{\max}$ we denote the maximum value of the reaction rate.

Herein, the following material parameters are used: $D_{CO_2} = 3.5$ cm^2/day, $D_{H_2O} = 1$ cm^2/day, $D_{Ca(OH)_2} = 0.864$ cm^2/day, $\lambda_{CO_2} = 58.9286 * 10^{-6}$g/cm^3, $\lambda_{Ca(OH)_2} = 0.077$g/cm^3, $\lambda_{H_2O} = 1$g/cm^3, $\eta_{\max} = k\lambda_{CO_2}^p \lambda_{Ca(OH)_2}^q$, where $k = 150$ [1/day*(g/cm^3)$^{1-p-q}$]. Moreover, we fix $p = 2$ and $q = 1$ but other choices are possible as well. By (5.6), we have $\beta(p) = \frac{p-1}{2(p+1)}$, and hence, we expect results which are asymptotically insensitive with respect to the selection of the partial-reaction order q. Since we are in the fast reaction *vs.* slow diffusion case, we expect that asymptotically the overall influence of the exponents p and q on the concentration

profiles and position of the reaction front is negligible [3]. These parameters define the following dimensionless numbers:

$$\beta_u := 1,\ \beta_v := \frac{\lambda_{\mathrm{Ca(OH)_2}}}{\lambda_{\mathrm{CO_2}}},\ \beta_w := \frac{\lambda_{\mathrm{H_2O}}}{\lambda_{\mathrm{CO_2}}}, \tag{8.1}$$

and

$$\delta_u := 1,\ \delta_v := \frac{D_{\mathrm{Ca(OH)_2}}}{D_{\mathrm{CO_2}}},\ \delta_w := \frac{D_{\mathrm{H_2O}}}{D_{\mathrm{CO_2}}}. \tag{8.2}$$

For simulations, we choose $\epsilon = 10^{-2}$ to scale the length variable and the characteristic time of CO_2 diffusion to scale the time variable. With these notations, the Thiele modulus reads

$$\Phi^2 := \frac{\eta_{\max}\epsilon^2}{D_{\mathrm{CO_2}}\lambda_{\mathrm{CO_2}}}. \tag{8.3}$$

Thorough discussions of the role of these dimensionless numbers are given in [26] and in appendix A of [23].

In the sequel, our focus is on calculating the asymptotic profiles of the involved active concentrations and of the asymptotic reaction front position. We begin with the next elementary observation: After a sufficient large time, the behavior of u within the diffusion layer is described via

$$u_\tau - \delta_u u_{zz} = 0 \text{ in } \mathbb{R}, t > 0, \tag{8.4}$$

$$u(z,0) = H(z),\ u(-\infty,\tau) = 0,\ u(\infty,\tau) = 1. \tag{8.5}$$

The system (8.4)-(8.5) admits the exact similarity solution

$$u(z,\tau) = \frac{1}{2}\left(1 + \mathrm{erf}\left(\frac{z}{2\sqrt{\beta_u \tau}}\right)\right).$$

In terms of (ζ,τ) variables, the latter equation reads

$$u(\zeta,\tau) = \frac{1}{2}\left[1 + \mathrm{erf}\left(\frac{1}{\sqrt{\beta_u}}(\zeta - m)\right)\right]. \tag{8.6}$$

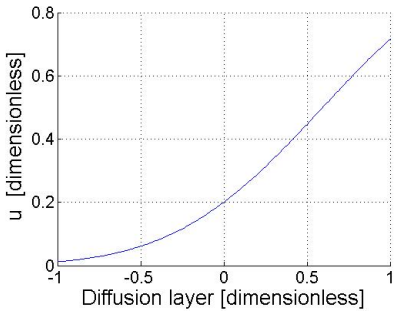

FIGURE 3. Profile of CO_2 vs. space within the diffusion layer.

Simultaneously, by the maximum principle the profile of w vanishes in the same region. The profile of u cf. (8.6) is shown in Fig. 3. It shows the tendency of CO_2 to decay near the reaction layer.

In the sequel, we want to obtain the asymptotic profiles of concentrations in the reaction layer. In order to obtain them, we need to solve the non-linear system

[3]For $p = 2$, (5.6) shows that ϵ is of order of $\mathcal{O}\left(\tau^{\frac{1}{6}}\right)$ which is negligible compared to the width of Ω_L. Following the same arguments, if $p = 1.5$, then $\epsilon \sim \mathcal{O}\left(\tau^{\frac{1}{10}}\right)$. Interestingly, if $p = 1$, then ϵ and τ appears to be asymptotically independent, while $\beta(p) \to \frac{1}{2}$ as $p \to \infty$.

of differential equations (7.1)-(7.6), which is described in section 7. It is worth mentioning that in [26] the effect of the reaction layer on the whole process was neglected. The approximation of the solution to the boundary-value problem (7.1),

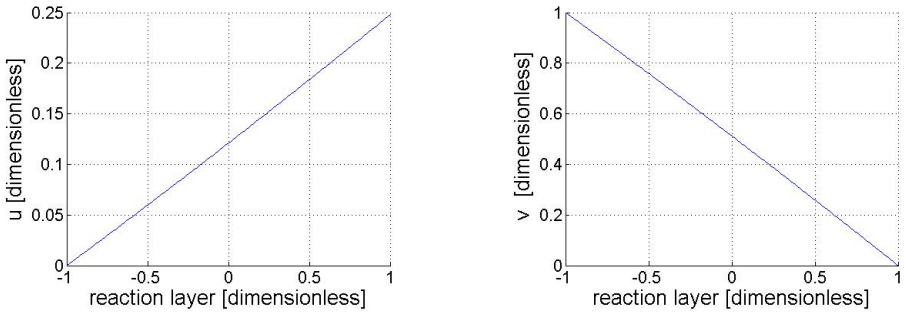

(a) (b)

FIGURE 4. (a)+(b) CO_2 and $Ca(OH)_2$ profiles vs. space. The reaction front propagates from right to left.

(7.4) and (7.11) is obtained by means of the code `bvp4c`, which is available in MATLAB, using default tolerances. To this end, the problem has to be transformed to first order form. The routine is based on both the collocation method and continuation argument, and is illustrated in [30] (chapter 3.2), e.g. Shooting methods can be an alternative to our strategy, see [33] or [20], e.g. More mathematical details on the application of the collocation method for two-points BVP can be found in [1], e.g. The numerical approximation of the reactant profiles in Fig. 4 is done within the reaction front. Firstly, we approximate the value of m for a given set of parameters by solving (7.8) in MATLAB by means of the routine `fminsearch`. The profile of u is depicted in Fig. 4 (a), while that of v is shown in Fig. 4 (b). In Fig. 5, we note a localized production of water which may be interpreted as a *barrier*. By *barrier* we simply mean that the water may locally fill the air part of some pores. On this way, the *water barrier* impedes the penetration of gaseous CO_2 and may lead to a slow down of the process or even to its stopping.

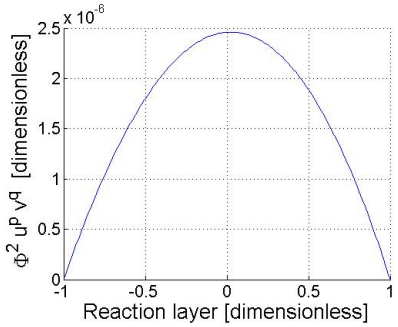

FIGURE 5. Plot of the reaction rate of $\Phi^2\hat{\mathcal{U}}^p\hat{\mathcal{V}}^q$ vs. space within the reaction layer. It points out a local production of water.

Asymptotically, the reaction front diffuses into the material with the speed

$$\sigma'(\tau) := -\frac{m}{\sqrt{2\tau}}, \tag{8.7}$$

see Fig. 7 (a) for a plot of the (asymptotical) interface position with respect to time compared with the experimental penetration depth measured by Bunte [5].

In Fig.7 (a) we also compare the position of the reaction front given by (2.9) with that respecting the law

$$\sigma(\tau) = -\sqrt{\frac{2\lambda_c D_{\mathrm{CO}_2}\tau}{\lambda_h}}, \tag{8.8}$$

which is basically the law proposed by Papadakis *et al.* [26] applied to this reaction-diffusion scenario. The results are comparable. For the chosen parameter set, our approach seems to be better[4]. The velocity of the front is plotted in Fig. 7 (b).

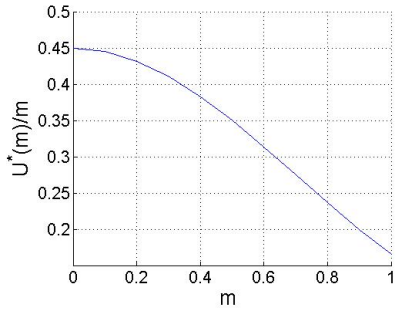

FIGURE 6. Behavior of $\frac{U^*(m)}{m}$ vs. m.

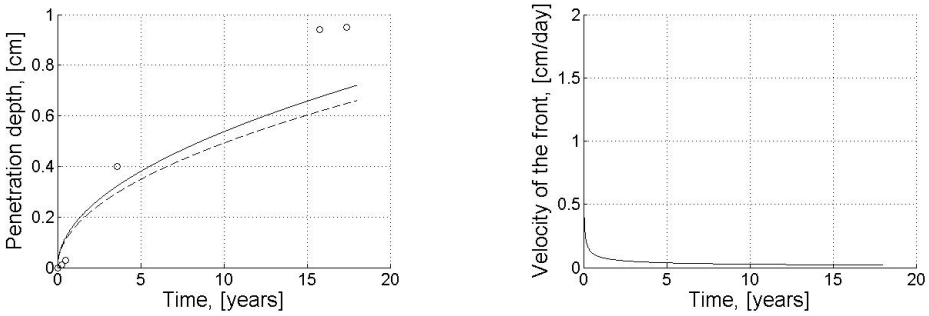

(a) (b)

FIGURE 7. (a) The solid line shows the interface position cf. (2.9) vs. time. The dashed line show the interface position cf. (8.8) vs. time. The points "∘" denote the measured penetration depths from [5]. (b) Plot of the velocity (8.7) of the front.

9. Discussion

There is no *explicit dependence*[5] of m defined cf. (7.8) on important material parameters like the curing time, degree of hydration, water-to-cement ratio, chemistry of the concrete and so on. Therefore, the criticism with respect to the asymptotic penetration law proposed in [26], which was addressed among others by Chaussadent [7] in his survey on concrete carbonation issues, can be repeated here as well. There are many arguments *pro et contra*. We do not dwell with them here, but mention that, at any rate, the merit of such an asymptotic approach is that it eliminates any fitting argument when determining the position of the reaction

[4]This is not yet concluding. More *qualitative* investigations are needed.

[5]However, the scaling parameters connect m with the initial and boundary data.

front. Namely, in our case we obtain the unknown parameter m as solution of a system of differential equations coupled with an algebraic one. The information concerning the chemistry of the concrete sample and the boundary conditions is comprised in the scaling parameters. Therefore, the asymptotic penetration law only depends on the choice of scaling parameters and that of m. Our asymptotic penetration depths are somehow close to those obtained by Papadakis *et al.* [26]. It is not clear whether we overestimate or underestimate their results.

Exploiting (7.8), we note that $\frac{U^*(m)}{m} = \mathcal{O}\left(\frac{1}{\Phi^2}\right)$. This can be interpreted in the following way: For increasing m, the fraction $\frac{U*(m)}{m}$ decreases, see Fig. 6. This also corresponds to increasing Thiele modulus Φ^2 and finally leads cf. (2.9) to higher penetration depths. Simple dimensional investigation shows that the proportionality constant c from

$$\frac{U^*(m)}{m} = c\Phi^2 \tag{9.1}$$

depends on the effective diffusion coefficient of CO_2 in air, maximum reaction rate, choice of length scale and initial concentration of $Ca(OH)_2$ in concrete. If m is known, then by (7.8) the constant c can be exactly computed. In this case, we have

$$c = \frac{D_{CO_2}\lambda_{Ca(OH)_2}}{\eta_{\max}\epsilon^2}, \tag{9.2}$$

where ϵ represents the characteristic length scale of interest. Furthermore, for certain values of m, we notice the linear behavior $\Phi^2(m) \approx \xi m$, where the approximate proportionality factor ξ can be calculated from Fig. 6 with the routine `diff` of MATLAB.

If we change the set of scaling parameters, then the main output (i.e. penetration depth vs. time plot) alters. More dimensional investigations and numerical simulations are needed in order to be able to identify the effect of each of the dimensionless parameters and dimensional length and time scales on the penetration depths. we will treat these aspects in a forthcoming publication.

At least two complementary research directions emerge from the preliminary character of this study. From one hand, the matched asymptotic analysis can be extended to tackle rather complex scenarios in which *several* reactive species can diffuse and admit *various structures of reaction kinetics*. Typically, tedious calculations become unavoidable. The paper [4] and this note give a basis for investigations in this direction. Note also that at this stage, the asymptotic results may intimately combine with numerics. On the other hand, the matched asymptotic analysis provides theoretical hints about the large-time behavior of concentration profiles and penetration front position, at least in the case when the front is thin but does not shrink to a sharp interface. There are essential differences between the asymptotic behavior of moving thin fronts and sharp interfaces, see corresponding remarks in [22, 10, 9, 31, 11], e.g., where the exact asymptotic behavior is shown to be strongly dependent on the structure of the reaction kinetics and type of the moving front (sharp interface or not). This first step gives us additional motivation to reconsider at a later stage the moving-interface approach to carbonation as stated in [23, 24].

The present asymptotic approach is purely formal. It needs to be cast in a proper mathematical framework. At this moment, it is not quite clear how this framework should look like, especially if also we think of recovering the sharp interface scenario.

Appendix A. The choice of scaling exponents

In this appendix, we discuss the elimination procedure of the traveling-wave solutions and of the other non-relevant situations which may occur as result of

the scaling of the reaction front, see section 3. To this end, we solve systems of linear algebraic inequalities. Our investigation follows [4] and essentially uses the weak coupling between the mass-balance equation of moisture and the rest of mass balance equations.

We proceed in the following manner:

Because of $\gamma = \frac{1}{p-1}$, the case (U3) is incompatible with both (V1) and (V2). Therefore all combinations containing (U3) have to be discarded.

If $\nu = \gamma$, then the latter assertion holds for (W3), too.

Obviously, in the case (V1) we have $\gamma = \frac{1}{p}$. This fact does not match the cases (U1), (U2) and (U3).

Gathering together these incompatibilities between the scaling exponents, we see that a successful configuration can only involve (U1), (U2), (V2), (W1) and (W2).

We note that there is a certain incompatibility between the cases (U2) and (V2) [and also (W2)]. Namely, from $\alpha - \beta + \gamma(p-1) - 1 = 0$ and $\alpha - \beta + \gamma p - 1 = 0$, we deduce that $\gamma = 0$. This contradicts our choice of γ.

The triple (U1, V2, W1) is the successful combination. Notice that $\gamma \leq \frac{1}{p-1}$. From $\alpha - \frac{\gamma}{2}(p-1) \leq 0$ and $\gamma(p-1) = 2\beta$, we obtain that $\alpha \leq \frac{1}{2}$ and $\beta \leq \frac{1}{2}$. The rest of the discussion follows as in [4].

Acknowledgments

The authors acknowledge financial support from the DFG grant SPP 1122 *Prediction of the course of physicochemical damage processes involving mineral materials*. They also thank S. Meier (University of Bremen) for improving a preliminary version of the manuscript.

References

1. U. M. Asher, R. M. M. Mattheij, and R. D. Russell, *Numerical solution of boundary value problems for ordinary differential equations*, Classics in Applied Mathematics, SIAM, Philadelphia, 1995.
2. G. I. Barenblatt, *Similarity, self-similarity, and intermediate asymptotics*, Consultants Bureau, NY, London, 1979.
3. ———, *Dimensional analysis*, Gordon and Breach Publishers, NY, 1987.
4. M. Z. Bazant and H. A. Stone, *Asymptotics of reaction-diffusion fronts with one static and one diffusing reactant*, Physica D **147** (2000), 95–121.
5. D. Bunte, *Zum Karbonatisierungsbedingten Verlust der Dauerhaftigkeit von Außenbauteilen aus Stahlbeton*, Ph.D. thesis, TU Braunschweig, 1994.
6. J.H. Cahyadi and T. Uomoto, *Influence of environmental relative humidity on carbonation of concrete (mathematical modeling)*, Durability of Building Materials and Components (Omiya, Japan), vol. 6, 1993, pp. 1142–1151.
7. T. Chaussadent, *États de lieux et réflexions sur la carbonatation du beton armé*, Tech. Report OA 29, Laboratoire Central de Ponts et Chaussées, Paris, 1999.
8. D. D. Do, *On the validity of the shrinking core model in non-catalytic gas-solid reactions*, Chem. Eng. Sci. **37** (1982), 1477–1481.
9. H. Emmerich, *The diffuse interface approach in material sciences*, Physics and Astronomy, vol. m 73, Springer Verlag, Berlin, 2003.
10. P. C. Fife, *Dynamics of internal layers and diffusive interfaces*, CMBS-NSF Regional Conference Series in Applied Mathematics, SIAM, Philadelphia, Pennsylvania, 1988.
11. M. Fila and Ph. Souplet, *Existence of global solutions with slow decay and unbounded free boundary for a superlinear stefan problem*, Interfaces and Free Boundaries **3** (2001), 337–344.
12. E. J. Hinch, *Perturbation methods*, Cambridge Texts in Applied Mathematics, Cambridge University Press, Cambridge, 1991.
13. Y. Houst and F. H. Wittmann P. Roelfstra, *A model to predict service life of concrete structures*, Proc. Int. Conf. Techn. Akademie Esslingen, 1983, pp. 181–186.
14. J. Kropp, *Relations between transport characteristics and durability*, Performance Criteria for Concrete Durability (J. Kropp and H. K. Hilsdorf, eds.), RILEM Report 12, E and FN Spon Editions, 1995, pp. 97–137.

15. C. Leger, F. Argoul, and M. Z. Bazant, *Front dynamics during diffusion-limited corrosion of ramified electrodeposits*, J. Phys. Chem. B **103** (1999), 5841–5851.
16. C. C. Lin and L. A. Segel, *Mathematics applied to deterministic problems in the natural sciences*, Classics in Applied Mathematics, SIAM, Philadelphia, 1988.
17. J. D. Logan, *Transport modeling in hydrogeochemical systems*, Interdisciplinary Applied Mathematics, vol. 17, Springer Verlag, NY, Berlin, Heidelberg, Barcelona, Hong Kong, London, Milan, Paris, Singapore, Tokyo, 2001.
18. M. Mainguy, *Modèles de diffusion non-linéaires en millieux poreux. application à la dissolution et au séchage des matériaux cimentaires*, Thése de doctorat, École Nationale des Ponts et Chaussées, 1999.
19. M. Mainguy and O. Coussy, *Propagation fronts during calcium leaching and chloride penetration*, ASCE J. Engng. Mech. **3** (2000), 252–257.
20. V. Martinez, A. Marquina, and R. Donat, *Shooting methods for one-dimensional diffusion-absorption problems*, SIAM J. Numer. Anal. **31** (1994), no. 2, 572–589.
21. S. A. Meier, M. A. Peter, A. Muntean, and M. Böhm, *Modelling and simulation of concrete carbonation with internal layers*, Berichte aus der Technomathematik 05-02, ZeTeM, University of Bremen, 2005.
22. A. Muntean, *Modeling reaction zones as free boundaries*, unpublished manuscript, ZeTeM, Fachbereich Mathematik, University of Bremen, 2006.
23. ———, *A moving-boundary problem: Modeling, analysis and simulation of concrete carbonation*, Ph.D. thesis, Faculty of Mathematics,University of Bremen, Cuvillier Verlag, Göttingen, Germany, 2006.
24. A. Muntean and M. Böhm, *Dynamics of a moving reaction interface in a concrete wall*, Free and Moving Boundary Problems. Theory and Applications (I. N. Figuiredo J. F Rodrigues, L. Santos, ed.), International Series of Numerical Mathematics, vol. 154, Birkhäuser, Basel, 2006, pp. 317–326.
25. A. Muntean, S. Meier, M. Peter, M. Böhm, and J. Kropp, *A note on the limitations of the use of accelerated concrete-carbonation tests for service-life predictions*, Tech. Report 05-04, ZeTeM, University of Bremen, 2005.
26. V. G. Papadakis, C. G. Vayenas, and M. N. Fardis, *A reaction engineering approach to the problem of concrete carbonation*, AIChE Journal **35** (1989), 1639.
27. A. V. Saetta, B. A. Schrefler, and R. V. Vitaliani, *The carbonation of concrete and the mechanism of moisture, heat and carbon dioxide flow through porous materials*, Cement and Concrete Research **23** (1993), no. 4, 761–772.
28. A. Schenkel, P. Wittwer, and J. Stubbe, *Asymptotics of solutions in an $A + B \to C$ reaction-diffusion system*, Physica D **69** (1993), 135–147.
29. L. I. Sedov, *A course in continuum mechanics*, vol. 2. Physical foundations and formulations of problems, Wolters-Noordoff Publishing, Groningen, 1972.
30. L. E. Shampine, I. Gladwell, and S. Thompson, *Solving odes with matlab*, Cambridge University Press, 2003.
31. Ph. Souplet, Ghidousche H., and Tarzia D., *Decay of global solutions, stability and blow-up for a reaction-diffusion problem with free boundary*, Proc. Amer. Math. Soc. **129** (2001), 781–792.
32. A. Steffens, *Modellierung von karbonatisierung und chloridbindung zur numerischen analyse der korrosionsgefaehrdung der betonbewehrung*, Dissertation, Institut für Statik Technische Universität Braunschweig, 2000.
33. J. Stoer and R. Bulirsch, *Numerische Mathematik*, 3 ed., vol. 2, Springer Verlag, Berlin, 1990.
34. A. B. Tayler, *Mathematical models in applied mechanics*, Oxford Applied Mathematics and Computing Science Series, Clarendon Press, Oxford, 1986.
35. M. Thiéry, *Modélisation de la carbonatation atmosphérique des materiaux cimentaires*, Tech. Report OA 52, Laboratoire Central des Ponts et Chaussées, Paris, 2005.
36. A. Yen, A. L. Liu, L. Koo, B. Vilensky, H. Taitelbaum, and R. Kopelman, *Spatiotemporal patterns and nonclassical kinetics of competing elementary reactions: chronium complex formation with xylenol orange in a capillary*, J. Phys. Chem. A **101** (1997), 2819–2827.

Centre for Industrial Mathematics, Department of Mathematics and Computer Science, FB 3, Postfach 330440, University of Bremen, 28334, Bremen, Germany, e-mail: {muntean,mbohm}@math.uni-bremen.de

Berichte aus der Technomathematik ISSN 1435-7968

http://www.math.uni-bremen.de/zetem/berichte.html

— Vertrieb durch den Autor —

Reports **Stand: 12. September 2006**

98–01. Peter Benner, Heike Faßbender:
An Implicitly Restarted Symplectic Lanczos Method for the Symplectic Eigenvalue Problem, Juli 1998.

98–02. Heike Faßbender:
Sliding Window Schemes for Discrete Least-Squares Approximation by Trigonometric Polynomials, Juli 1998.

98–03. Peter Benner, Maribel Castillo, Enrique S. Quintana-Ortí:
Parallel Partial Stabilizing Algorithms for Large Linear Control Systems, Juli 1998.

98–04. Peter Benner:
Computational Methods for Linear–Quadratic Optimization, August 1998.

98–05. Peter Benner, Ralph Byers, Enrique S. Quintana-Ortí, Gregorio Quintana-Ortí:
Solving Algebraic Riccati Equations on Parallel Computers Using Newton's Method with Exact Line Search, August 1998.

98–06. Lars Grüne, Fabian Wirth:
On the rate of convergence of infinite horizon discounted optimal value functions, November 1998.

98–07. Peter Benner, Volker Mehrmann, Hongguo Xu:
A Note on the Numerical Solution of Complex Hamiltonian and Skew-Hamiltonian Eigenvalue Problems, November 1998.

98–08. Eberhard Bänsch, Burkhard Höhn:
Numerical simulation of a silicon floating zone with a free capillary surface, Dezember 1998.

99–01. Heike Faßbender:
The Parameterized SR Algorithm for Symplectic (Butterfly) Matrices, Februar 1999.

99–02. Heike Faßbender:
Error Analysis of the symplectic Lanczos Method for the symplectic Eigenvalue Problem, März 1999.

99–03. Eberhard Bänsch, Alfred Schmidt:
Simulation of dendritic crystal growth with thermal convection, März 1999.

99–04. Eberhard Bänsch:
Finite element discretization of the Navier-Stokes equations with a free capillary surface, März 1999.

99–05. Peter Benner:
Mathematik in der Berufspraxis, Juli 1999.

99–06. Andrew D.B. Paice, Fabian R. Wirth:
Robustness of nonlinear systems and their domains of attraction, August 1999.

99–07. Peter Benner, Enrique S. Quintana-Ortí, Gregorio Quintana-Ortí:
Balanced Truncation Model Reduction of Large-Scale Dense Systems on Parallel Computers, September 1999.

99–08. Ronald Stöver:
Collocation methods for solving linear differential-algebraic boundary value problems, September 1999.

99–09. Huseyin Akcay:
Modelling with Orthonormal Basis Functions, September 1999.

99–10. Heike Faßbender, D. Steven Mackey, Niloufer Mackey:
Hamilton and Jacobi come full circle: Jacobi algorithms for structured Hamiltonian eigenproblems, Oktober 1999.

99–11. Peter Benner, Vincente Hernández, Antonio Pastor:
On the Kleinman Iteration for Nonstabilizable System, Oktober 1999.

99–12. Peter Benner, Heike Faßbender:
A Hybrid Method for the Numerical Solution of Discrete-Time Algebraic Riccati Equations, November 1999.

99–13. Peter Benner, Enrique S. Quintana-Ortí, Gregorio Quintana-Ortí:
Numerical Solution of Schur Stable Linear Matrix Equations on Multicomputers, November 1999.

99–14. Eberhard Bänsch, Karol Mikula:
Adaptivity in 3D Image Processing, Dezember 1999.

00–01. Peter Benner, Volker Mehrmann, Hongguo Xu:
Perturbation Analysis for the Eigenvalue Problem of a Formal Product of Matrices, Januar 2000.

00–02. Ziping Huang:
Finite Element Method for Mixed Problems with Penalty, Januar 2000.

00–03. Gianfrancesco Martinico:
Recursive mesh refinement in 3D, Februar 2000.

00–04. Eberhard Bänsch, Christoph Egbers, Oliver Meincke, Nicoleta Scurtu:
Taylor-Couette System with Asymmetric Boundary Conditions, Februar 2000.

00–05. Peter Benner:
Symplectic Balancing of Hamiltonian Matrices, Februar 2000.

00–06. Fabio Camilli, Lars Grüne, Fabian Wirth:
A regularization of Zubov's equation for robust domains of attraction, März 2000.

00–07. Michael Wolff, Eberhard Bänsch, Michael Böhm, Dominic Davis:
Modellierung der Abkühlung von Stahlbrammen, März 2000.

00–08. Stephan Dahlke, Peter Maaß, Gerd Teschke:
Interpolating Scaling Functions with Duals, April 2000.

00–09. Jochen Behrens, Fabian Wirth:
A globalization procedure for locally stabilizing controllers, Mai 2000.

00–10. Peter Maaß, Gerd Teschke, Werner Willmann, Günter Wollmann:
Detection and Classification of Material Attributes – A Practical Application of Wavelet Analysis, Mai 2000.

00–11. Stefan Boschert, Alfred Schmidt, Kunibert G. Siebert, Eberhard Bänsch, Klaus-Werner Benz, Gerhard Dziuk, Thomas Kaiser:
Simulation of Industrial Crystal Growth by the Vertical Bridgman Method, Mai 2000.

00–12. Volker Lehmann, Gerd Teschke:
Wavelet Based Methods for Improved Wind Profiler Signal Processing, Mai 2000.

00–13. Stephan Dahlke, Peter Maass:
A Note on Interpolating Scaling Functions, August 2000.

00–14. Ronny Ramlau, Rolf Clackdoyle, Frédéric Noo, Girish Bal:
Accurate Attenuation Correction in SPECT Imaging using Optimization of Bilinear Functions and Assuming an Unknown Spatially-Varying Attenuation Distribution, September 2000.

00–15. Peter Kunkel, Ronald Stöver:
Symmetric collocation methods for linear differential-algebraic boundary value problems, September 2000.

00–16. Fabian Wirth:
The generalized spectral radius and extremal norms, Oktober 2000.

00–17. Frank Stenger, Ahmad Reza Naghsh-Nilchi, Jenny Niebsch, Ronny Ramlau:
A unified approach to the approximate solution of PDE, November 2000.

00–18. Peter Benner, Enrique S. Quintana-Ortí, Gregorio Quintana-Ortí:
Parallel algorithms for model reduction of discrete–time systems, Dezember 2000.

00–19. Ronny Ramlau:
A steepest descent algorithm for the global minimization of Tikhonov–Phillips functional, Dezember 2000.

01–01. Efficient methods in hyperthermia treatment planning:
Torsten Köhler, Peter Maass, Peter Wust, Martin Seebass, Januar 2001.

01–02. Parallel Algorithms for LQ Optimal Control of Discrete-Time Periodic Linear Systems:
Peter Benner, Ralph Byers, Rafael Mayo, Enrique S. Quintana-Ortí, Vicente Hernández, Februar 2001.

01–03. Peter Benner, Enrique S. Quintana-Ortí, Gregorio Quintana-Ortí:
Efficient Numerical Algorithms for Balanced Stochastic Truncation, März 2001.

01–04. Peter Benner, Maribel Castillo, Enrique S. Quintana-Ortí:
Partial Stabilization of Large-Scale Discrete-Time Linear Control Systems, März 2001.

01–05. Stephan Dahlke:
Besov Regularity for Edge Singularities in Polyhedral Domains, Mai 2001.

01–06. Fabian Wirth:
A linearization principle for robustness with respect to time-varying perturbations, Mai 2001.

01–07. Stephan Dahlke, Wolfgang Dahmen, Karsten Urban:
Adaptive Wavelet Methods for Saddle Point Problems - Optimal Convergence Rates, Juli 2001.

01–08. Ronny Ramlau:
Morozov's Discrepancy Principle for Tikhonov regularization of nonlinear operators, Juli 2001.

01–09. Michael Wolff:
Einführung des Drucks für die instationären Stokes–Gleichungen mittels der Methode von Kaplan, Juli 2001.

01–10. Stephan Dahlke, Peter Maaß, Gerd Teschke:
Reconstruction of Reflectivity Desities by Wavelet Transforms, August 2001.

01–11. Stephan Dahlke:
Besov Regularity for the Neumann Problem, August 2001.

01–12. Bernard Haasdonk, Mario Ohlberger, Martin Rumpf, Alfred Schmidt, Kunibert G. Siebert:
h–p–Multiresolution Visualization of Adaptive Finite Element Simulations, Oktober 2001.

01–13. Stephan Dahlke, Gabriele Steidl, Gerd Teschke:
Coorbit Spaces and Banach Frames on Homogeneous Spaces with Applications to Analyzing Functions on Spheres, August 2001.

02–01. Michael Wolff, Michael Böhm:
Zur Modellierung der Thermoelasto-Plastizität mit Phasenumwandlungen bei Stählen sowie der Umwandlungsplastizität, Februar 2002.

02–02. Stephan Dahlke, Peter Maaß:
An Outline of Adaptive Wavelet Galerkin Methods for Tikhonov Regularization of Inverse Parabolic Problems, April 2002.

02–03. Alfred Schmidt:
A Multi-Mesh Finite Element Method for Phase Field Simulations, April 2002.

02–04. Sergey N. Dachkovski, Michael Böhm:
A Note on Finite Thermoplasticity with Phase Changes, Juli 2002.

02–05. Michael Wolff, Michael Böhm:
Phasenumwandlungen und Umwandlungsplastizität bei Stählen im Konzept der Thermoelasto-Plastizität, Juli 2002.

02–06. Gerd Teschke:
Construction of Generalized Uncertainty Principles and Wavelets in Anisotropic Sobolev Spaces, August 2002.

02–07. Ronny Ramlau:
TIGRA – an iterative algorithm for regularizing nonlinear ill–posed problems, August 2002.

02–08. Michael Lukaschewitsch, Peter Maaß, Michael Pidcock:
Tikhonov regularization for Electrical Impedance Tomography on unbounded domains, Oktober 2002.

02–09. Volker Dicken, Peter Maaß, Ingo Menz, Jenny Niebsch, Ronny Ramlau:
Inverse Unwuchtidentifikation an Flugtriebwerken mit Quetschöldämpfern, Oktober 2002.

02–10. Torsten Köhler, Peter Maaß, Jan Kalden:
Time-series forecasting for total volume data and charge back data, November 2002.

02–11. Angelika Bunse-Gerstner:
A Short Introduction to Iterative Methods for Large Linear Systems, November 2002.

02–12. Peter Kunkel, Volker Mehrmann, Ronald Stöver:
Symmetric Collocation for Unstructured Nonlinear Differential-Algebraic Equations of Arbitrary Index, November 2002.

02–13. Michael Wolff:
Ringvorlesung: Distortion Engineering 2
Kontinuumsmechanische Modellierung des Materialverhaltens von Stahl unter Berücksichtigung von Phasenumwandlungen, Dezember 2002.

02–14. Michael Böhm, Martin Hunkel, Alfred Schmidt, Michael Wolff:
Evaluation of various phase-transition models for 100Cr6 for application in commercial FEM programs, Dezember 2002.

03–01. Michael Wolff, Michael Böhm, Serguei Dachkovski:
Volumenanteile versus Massenanteile - der Dilatometerversuch aus der Sicht der Kontinuumsmechanik, Januar 2003.

03–02. Daniel Kessler, Ricardo H. Nochetto, Alfred Schmidt:
A posteriori error control for the Allen-Cahn Problem: circumventing Gronwall's inequality, März 2003.

03–03. Michael Böhm, Jörg Kropp, Adrian Muntean:
On a Prediction Model for Concrete Carbonation based on Moving Interfaces - Interface concentrated Reactions, April 2003.

03–04. Michael Böhm, Jörg Kropp, Adrian Muntean:
A Two-Reaction-Zones Moving-Interface Model for Predicting $Ca(OH)_2$ Carbonation in Concrete, April 2003.

03–05. Vladimir L. Kharitonov, Diederich Hinrichsen:
Exponential estimates for time delay systems, May 2003.

03–06. Michael Wolff, Michael Böhm, Serguei Dachkovski, Günther Löwisch:
Zur makroskopischen Modellierung von spannungsabhängigem Umwandlungsverhalten und Umwandlungsplastizität bei Stählen und ihrer experimentellen Untersuchung in einfachen Versuchen, Juli 2003.

03–07. Serguei Dachkovski, Michael Böhm, Alfred Schmidt, Michael Wolff:
Comparison of several kinetic equations for pearlite transformation in 100Cr6 steel,
Juli 2003.

03–08. Volker Dicken, Peter Maass, Ingo Menz, Jenny Niebsch, Ronny Ramlau:
Nonlinear Inverse Unbalance Reconstruction in Rotor dynamics,
Juli 2003.

03–09. Michael Böhm, Serguei Dachkovski, Martin Hunkel, Thomas Lübben, Michael Wolff:
Übersicht über einige makroskopische Modelle für Phasenumwandlungen im Stahl,
Juli 2003.

03–10. Michael Wolff, Friedhelm Frerichs, Bettina Suhr:
Vorstudie für einen Bauteilversuch zur Umwandlungsplastizität bei der perlitischen Umwandlung des Stahls 100 Cr6,
August 2003.

03–11. Michael Wolff, Bettina Suhr:
Zum Vergleich von Massen- und Volumenanteilen bei der perlitischen Umwandlung der Stähle 100Cr6 und C80,
September 2003.

03–12. Rike Grotmaack, Adrian Muntean:
Stabilitätsanalyse eines Moving-Boundary-Modells der beschleunigten Karbonatisierung von Portlandzementen,
September 2003.

03–13. Alfred Schmidt, Michael Wolff, Michael Böhm:
Numerische Untersuchungen für ein Modell des Materialverhaltens mit Umwandlungsplastizität und Phasenumwandlungen beim Stahl 100Cr6 (Teil 1),
September 2003.

04–01. Liliana Cruz Martin, Gerd Teschke:
A new method to reconstruct radar reflectivities and Doppler information,
Januar 2004.

04–02. Ingrid Daubechies, Gerd Teschke:
Wavelet based image decomposition by variational functionals,
Januar 2004.

04–03. N. Guglielmi, F. Wirth, M. Zennaro:
Complex polytope extremality results for families of matrices,
März 2004.

04–04. I. Daubechies, G. Teschke:
Variational image restoration by means of wavelets: simultaneous decomposition, deblurring and denoising,
April 2004.

04–05. V.L. Kharitonov, E. Plischke:
Lyapunov matrices for time-delay systems,
April 2004.

04–06. Ronny Ramlau:
On the use of fixed point iterations for the regularization of nonlinear ill-posed problems,
Juni 2004.

04–07. Christof Büskens, Matthias Knauer:
Higher Order Real-Time Approximations In Optimal Control of Multibody-Systems For Industrial Robots,
August 2004.

04–08. Christof Büskens, Roland Griesse:
Computational Parametric Sensitivity Analysis of Perturbed PDE Optimal Control Problems with State and Control Constraints,
August 2004.

04–09. Christof Büskens:
Higher Order Real-Time Approximations of Perturbed Control Constrainted PDE Optimal Control Problems ,
August 2004.

04–10. Christof Büskens, Matthias Gerdts:
Differentiability of Consistency Functions,
August 2004.

04–11. Robert Baier, Christof Büskens, Ilyes Aïssa Chama, Matthias Gerdts:
Approximation of Reachable Sets by Direct Solution Methods of Optimal Control Problems,
August 2004.

04–12. J. Soares, G. Teschke, M. Zhariy:
A Wavelet Regularization for Nonlinear Diffusion Equations,
September 2004.

05–01. Alfred Schmidt, Adrian Muntean, Michael Böhm:
Numerical experiments with Self-Adaptive Finite Element Simulations in 2D for the Carbonation of Concrete,
April 2005.

05–02. Sebastian A. Meier, Malte A. Peter, Adrian Muntean, Michael Böhm:
Modelling and simulation of concrete carbonation with internal layers,
April 2005.

05–03. Malte A. Peter, Adrian Muntean, Sebastian A. Meier, Michael Böhm:
Modelling and simulation of concrete carbonation: competition of several carbonation reactions,
April 2005.

05–04. Adrian Muntean, Sebastian A. Meier, Malte A. Peter, Michael Böhm, Jörg Kropp:
A note on limitations of the use of accelerated concrete-carbonation tests for service-life predictions,
April 2005.

05–05. Sergey Dashkovskiy, Björn S. Rüffer, Fabian R. Wirth:
An ISS Small-Gain Theorem for General Networks,
Juni 2005.

06–01. Prof. Dr. Christof Büskens, Peter Lasch:
Suboptimal Improvement of the classical Riccati Controller,
März 2006.

06–02. Michael Wolff, Michael Böhm:
Transformation-induced plasticity in steel - general modelling, analysis and parameter identification,
April 2006.

06–03. Adrian Muntean, Michael Böhm:
A sharp-interface moving-boundary system modeling carbonation penetration in concrete,
April 2006.

06–04. Michael Wolff, Michael Böhm,Sebastian Meier:
Modellierung der Wechselwirkung von Kohlenstoff-Diffusion und ferritischen Phasenumwandlungen für einen untereutektoiden unlegierten Stahl,
Mai 2006.

06–05. Adrian Muntean:
Error bounds on a semi-discrete finite element approximation of the weak solution to a one phase moving-boundary system describing concrete carbonation,
Mai 2006.

06–06. Sergey Dashkovskiy, Björn S. Rüffer, Fabian R. Wirth:
Construction of ISS Lyapunov functions for networks,
Juli 2006.

06–07. Adrian Muntean and Michael Böhm:
Length scales in the concrete carbonation process and water barrier effect: a matched asymptotics approach,
September 2006.